

MOLECULAR ION RECOIL SPECTROSCOPY
APPLIED TO METHANE

by

VINCENT NEEDHAM
B.S., Kansas State University, 1982

A MASTER'S THESIS

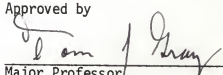
submitted in partial fulfillment of the
requirements for the degree

MASTER OF SCIENCE

Department of Physics
Kansas State University

1984

Approved by


Major Professor

LD
2668
.T4
1984
N43
C. 2

A11202 960469

TABLE OF CONTENTS

	Page
LIST OF FIGURES	iii
LIST OF TABLES	iv
ACKNOWLEDGEMENTS	v
Chapter	
I. INTRODUCTION	1
II. BACKGROUND	2
A. Molecular Ion Chemistry	2
B. Recoil Ion Sources	4
III. EXPERIMENT	6
IV. INTERPRETATION OF RESULTS	12
V. CONCLUSIONS AND PROSPECTS	39
APPENDIX A	41
APPENDIX B	52
REFERENCES	59
ABSTRACT	

LIST OF FIGURES

Figure		Page
1.	Experimental apparatus with detail of the recoil ion source	7
2.	Electronics used for coincidence measurements	10
3.	Recoil spectrum of CH_4 at a target gas pressure of 1.0 mtorr	13
4.	Synthetic spectrum based on model calculations	17
5.	Recoil spectrum of CH_4 at a target gas pressure of 0.5 mtorr	20
6.	Recoil spectrum of CH_4 at a target gas pressure of 4.0 mtorr	22
7.	Window 0, showing ions of the form CH_n^+	24
8.	Projection of primary ion locus from window 0	26
9.	Window 1, showing ions of the form CH_n^{2+} and CH_n^{3+}	28
10.	Projections of the primary ion locus and CH^{2+} locus from window 1	30
11.	Window 2, showing ions of the form CH_n^{2+} and CH_n^{3+}	33
12.	Projection of the C^{2+} locus from window 2	35
A1.	Schematic diagram of the ion source and analysis system. .	42

LIST OF TABLES

Table	Page
I. Examples of Postulated Events in Two-Dimensional Coincidence Spectra for CH ₄ Source Gas	16

ACKNOWLEDGEMENTS

This thesis is dedicated to my parents, whose love and support made it possible.

The greatest of thanks go to Drs. Tom Gray and James Legg for sharing their knowledge and enthusiasm.

Further thanks are due to Robert Krause, Mike Wells and the rest of the laboratory staff for their tireless work; to Kileen Himes for typing the manuscript and to Peter Seitz for assistance in reducing the data.

Finally, I would like to acknowledge the financial support of the U.S. Department of Energy, Division of Chemical Sciences.

Chapter I

INTRODUCTION

Experimental studies of chemistry on the atomic scale have been conducted since about 1925, yet in that time only a handful of doubly charged molecular ions have been observed and no molecules of any higher charge state have been found. Since the 1960's, physicists have been investigating the atomic collisions that can generate recoil ions of high charge state but very low kinetic energy. This phenomenon has been used since 1978 to generate beams of highly charged atomic ions. In order to study a highly charged molecular system, then, it seems natural to consider applying the recoil ion methods. It is the purpose of this thesis to present the technique of molecular ion recoil spectroscopy, which promises to be a powerful tool for the study of all molecular ions, their physics and their chemistry.

The first section of this work considers the previous findings in the area of molecular ion chemistry and also examines the development of the recoil ion source as a tool in physics. The current experiment, which examines the recoil ions of methane, is then described and the methods developed for interpreting spectra are explained. Lastly, prospects for the future application of molecular recoil ion spectroscopy are entertained.

Chapter II

BACKGROUND

A) Molecular Ion Chemistry

Most of the doubly charged molecular ions that have been seen are those of simple molecules where the doubly charged state is accessible via a Franck-Condon transition, i.e., a transition occurring without the rearrangement of the molecule's nuclei. Examples of such ions and their measured ionization energies can be found in the work of Agee, et al.¹ Many simple molecules cannot yield a doubly charged ion through such "vertical" transitions, however, and thus are not observable as products of the electron bombardment ion sources in common use. Electrons cannot impart the momentum necessary to rearrange the molecular geometry and thus permit a non-vertical transition. The case in point is that of methane, CH_4 .

In 1970, Spohr, et al.,² utilized the technique of Electron Spectroscopy for Chemical Analysis, or ESCA, in an attempt to measure the second ionization energy of CH_4 . They reported that CH_4^{2+} was being formed from electron bombardment and had a lifetime of approximately 10^{-15} s. In 1981, however, Ast, et al.³ reported the observation of CH_4^{2+} produced in the charge-stripping reaction $\text{CH}_4^+ + \text{N}_2 \rightarrow \text{CH}_4^{2+} + \text{R} + \text{e}$, where R and e were undetected residual products. This measurement utilized a ZAB mass spectrograph in the "reverse" geometry. In order to be detected the CH_4^{2+} ion must have a lifetime of ≈ 3 μs , the ion's transit time in the instrument. Rabrenovic, et al.⁴ later reported the observation of the fragmentation products CH_2^{2+} and C^{2+} resulting from the decay of CH_4^{2+} ions formed by charge stripping. Additionally, Litherland⁵ reported the observation of

metastable CH_2^{2+} molecules with a lifetime of 10 μs using accelerator based mass spectroscopy. No molecular ion of charge state greater than 2+ of any sort have heretofore been observed.

The observation of long-lived molecular ions prompted a reexamination of the theoretical molecular structure calculations for these ions. Hanner and Moran⁶ used an SCF-MO method to calculate the potential energy surface of CH_4^{2+} while also optimizing on the molecular geometry. This procedure revealed that vertical transitions from CH_4 to CH_4^{2+} were unstable, but that a multiple step ionization process (such as charge stripping provides) could produce a metastable ion. The calculations were in good quantitative agreement with the charge stripping measurements of ionization energy as well. Seigbahn⁷ and Pople, *et al.*⁸ later performed more sophisticated large basis set calculations confirming that a change in molecular symmetry from T_d (tetrahedral) to D_{4h} (square planar) explain the conflicts between ESCA and the charge-stripping measurements.

These calculations predicted a minimum in the molecular potential for CH_4^{2+} which could account for the suggested experimental lifetimes of $\sim 3 \mu\text{s}$, hence ruling out the possibility that the short-lived state (10^{-15} s) was the only state that CH_4^{2+} could exist in. Pople, *et al.*⁸ also computed the molecular potential curves for CH^{2+} , CH_2^{2+} and CH_3^{2+} , with the predicted results that CH^{2+} had no minima in the potential curves while CH_3^{2+} had a very shallow minimum in its potential curve. Hence CH^{2+} should spontaneously decay because of the repulsive nature of the molecular potential while CH_3^{2+} should exhibit a very short lifetime. CH_2^{2+} was found to have a deeper minimum in the molecular potential and was thus predicted to have a lifetime of the same order as that observed for CH_4^{2+} . Heil, *et al.*⁹ calculated potential

curves for the $\text{CH}^{2+} \Sigma^+$ states which exhibit a shallow minimum at an inter-nuclear distance of approximately 3.2 bohr, which would allow a finite lifetime for the CH^{2+} molecule.

B) Recoil Ion Sources

The development and application of recoil ion sources is reviewed by Gray and Cocke.¹⁰ Briefly stated, collisions between fast heavy ions (an MeV/amu "pump beam") and target gases at large impact parameter may produce a low energy, highly charged (LEHQ) recoil ion. The observed recoil ion kinetic energy is typically ~ 1 eV, which means that the impact parameters involved in the ionization process are many times the K-shell radii. Charge states of the recoil ion available are generally a function of the pump beam; using 0.96 MeV/amu Cl^{12+} ions as a pump beam allows observation of Ne^{8+} recoils,¹¹ while 1.4 MeV/amu U^{44+} beams can generate bare Ne nuclei.¹²

The first direct observation of low velocity, heavy ions produced from targets bombarded by fast heavy ions was reported by Macfarlane and Torgerson.¹³ Fission fragments from a ^{252}Cf source were trained on a CsBr target evaporated onto a carbon backing and produced Cs^+ and Br^- ions with energies of ~ 8 eV. Edwards, et al.¹⁴ followed this work with the direct observation of charged molecular fragments coming from the dissociation of diatomic molecules (such as N_2) by 1 MeV H^+ and He^+ ions. This work concentrated on the energy spectra of the molecular fragments. Later work by the same group¹⁵ examined the dissociation of CH_4 by 1 MeV H^+ , He^+ , and O^+ projectiles. Continua observed in the C^{9+} and H^+ energy spectra led them to infer the existence of highly ionized CH_4 dissociating into said products.

The cross sections for LEHQ recoil production are large¹¹ ($\sim 10^{16} \text{ cm}^2$), therefore one can produce enough recoils to use as the beam in other experiments. This quality has already been exploited for studies of Auger and

x-ray spectra from recoils,¹⁶ for use with ion traps to measure charge exchange,¹⁷ for measuring charge exchange cross sections for recoil ion collisions with secondary target gases,¹⁸ and for measurements of energy gain in recoil-secondary target gas collision.¹⁹ The technique is applied here to the spectroscopy of molecular ions.

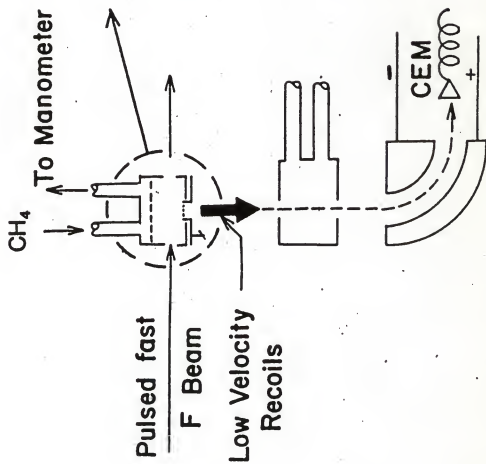
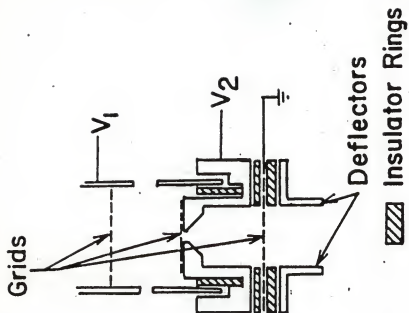
Chapter III

EXPERIMENT

This experiment was conducted at the James R. Macdonald Laboratory of the Kansas State University Department of Physics. The pump beam of 19 MeV F^{4+} ions was delivered by a 6 MV Tandem Van De Graaff accelerator. In order to perform time-of-flight (TOF) analysis on the recoil ions, the pump beam was pulsed with a typical repetition time of 16 μs and a typical pulse width of 10 ns. This provided a beam current of up to 10 nA, as read by a Faraday cup at the end of the beam line, about a meter downstream of the target gas cell.

The target gas cell, through which the pump beam passes, serves as the source of recoil ions and is illustrated in Figure 1. A target gas such as CH_4 is admitted into the cell and maintained at a pressure usually between 0.2 mtorr and 5.0 mtorr. The pressure was monitored by means of a capacitance manometer capable of measuring variations of hundredths of mtorr. To reduce interference from impurity ions in the spectra, ultra-high purity methane (99.99%) was used. The background pressure of the vacuum chamber was maintained at 4×10^{-7} torr. Molecular recoil ions are generated in collisions between the pump beam and the target gas. The recoils are swept out of the collision region by means of an electric field applied in two stages; a "pusher" grid and a focussing intermediate electrode. The applied voltages, labeled V_1 and V_2 in Figure 1, were typically +175 and +90 volts, respectively. This provided an accelerating voltage between the location of the pump beam and the final, grounded electrode of 150 volts. The beam

Figure 1. Experimental apparatus with detail of the recoil ion source.



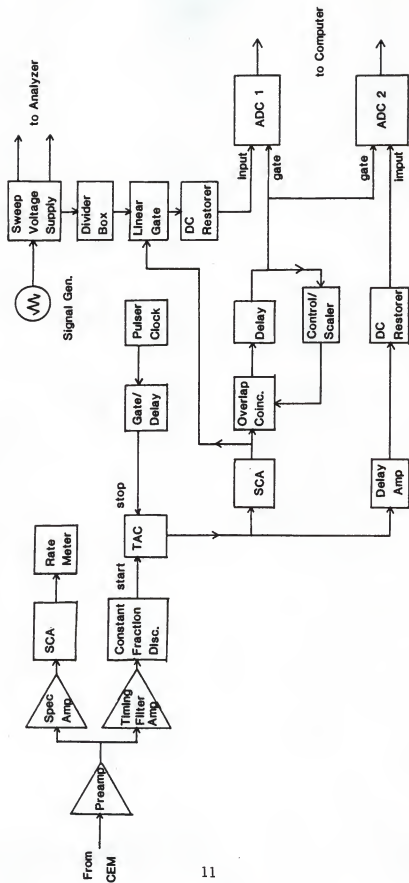
of recoil ions emerging from the cell could be steered using a set of horizontal and vertical deflectors immediately outside the cell.

The recoil ions were allowed to drift 10.7 cm after acceleration before encountering a secondary gas cell. This second cell was not used in the experiment; its 1 mm front aperture was used solely for collimation of the recoil ion beam. Having passed this second cell, the beam traverses a 90° double focussing hemispherical electrostatic analyzer whose electrodes are swept over a voltage range corresponding to beam energies from ~ 20 eV to ~ 550 eV. Those ions analyzed by the electric sector were detected in a channel electron multiplier (CEM) located 3.5 cm past the sector. The total drift length covered by the ions is 23.9 cm.

A detected ion's time of flight and the analyzer voltage at which it was passed was measured. The electronics required for the task are shown in Figure 2. The arrival of an ion in the CEM was used as the starting signal for a time-to-amplitude converter (TAC). The master clock output of the pump beam pulsing system was used as the stop signal. As a result of this arrangement, the time-of-flight scale on the final spectra reads from right to left. Typical times of flight through the complete apparatus are between 1 and 10 μ s.

A signal from the TAC, indicating the detection of an ion, was used to gate an output of the scanning analyzer voltage supply. The amplitude of this output was proportional to the scanner voltage. The scanner swept through the voltage range applied to the analyzer at a frequency of 4 Hz. The coincident time of flight and analyzer voltage signals were digitized and stored in a two-dimensional array in a PDP 11/34 computer using KSLIST multiparameter data acquisition software. The data was also stored on magnetic tape for later analysis.

Figure 2. Electronics used for coincidence measurements.



Chapter IV

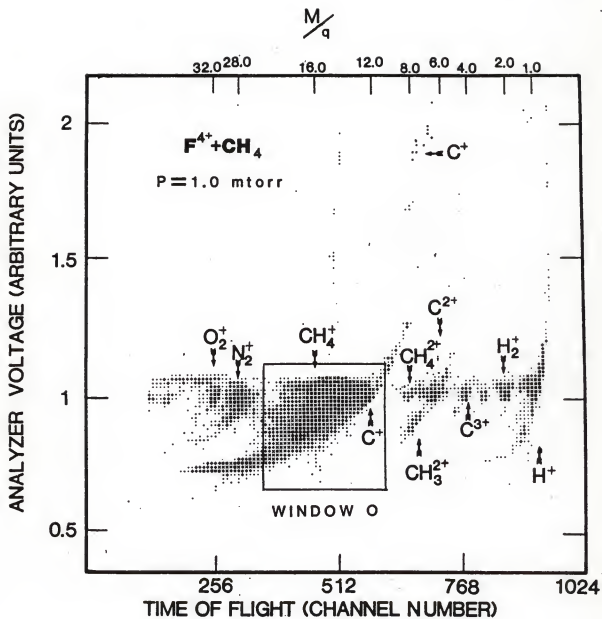
INTERPRETATION OF RESULTS

Figure 3 shows the two-dimensional coincidence spectrum of the recoil ions from CH_4 target gas at a pressure of 1 mtorr. The size and density of plotting symbols correspond to the number of events recorded in that area of the spectrum. It should be noted immediately that this and other spectra shown herein are highly compressed in both dimensions for purposes of display and do not reveal the full detail achievable by the technique. For a primary ion, i.e., a recoil ion formed at the pump beam and arriving unchanged at the detector, the time of flight depends on the square root of the mass to charge ratio of the ion, $\sqrt{M/q}$. The analyzer voltage is proportional to the ion's energy to charge ratio, E/q . The spectrum shown ranges in M/q from ~ 1 to ~ 50 and ranges in E from ~ 2 eV to ~ 550 eV.

These two-dimensional spectra are generally quite complex and very rich in detail; they are therefore difficult to interpret. To more easily identify the features seen in the spectrum a two-dimensional model was developed. This model considers the geometry of the recoil ion source and analyzer system, the voltages applied to the components of the system and the elementary physics of the various events that could occur to a given molecular or atomic ion species between the point of creation and that of detection. The derivation of this model and its BASIC language program code can be found in Appendices A and B, respectively.

Shown in Table I are various postulated events which might appear in a two-dimensional spectrum. The processes listed as examples in Table I may

Figure 3. Recoil spectrum of CH_4 at a target gas pressure of 1.0 mtorr.



take place while the ion is being accelerated in the recoil source or at any subsequent time during motion over the drift length between initial acceleration and final analysis and detection. Figure 4 presents a synthetic spectrum based on model calculations of these events.

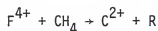
General features of the two dimensional coincidence spectra are as follows:

- (1) All primary ions are detected at a fixed analyzer voltage which is dependent upon the voltages applied to the recoil ion source and they arrive at the detector at times specified by $\sqrt{M/q}$.
- (2) Ions that have undergone charge exchange after acceleration arrive at the detector with the flight of time of the parent ion but require higher analyzer voltages which are proportional to the ratio of initial and final charge states, q_i/q_f .
- (3) Ions that have undergone charge exchange during acceleration will lie on a continuous locus determined by the time of flight and analyzer voltage with end points determined by the parent ion and final state ion.
- (4) Any ion detected as a distinct peak in the primary ion spectrum must have a lifetime $\tau \geq$ the flight time which is typically $\sim 3 \mu s$ in the present experimental apparatus.
- (5) Molecular ions with shorter lifetimes ($\tau =$ acceleration time, $\sim 0.2 \mu s$) may be detected as peaks in the spectrum, but such ions are found on the locus of points passing through the species to which they have decayed.
- (6) Ions that have increased their mass through a pickup reaction require lower analyzer voltages than the primary ions for passage through the electrostatic analyzer.
- (7) Ions that are the result of a Coulomb explosion near the site of

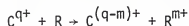
TABLE I

Examples of Postulated Events In Two-Dimensional
Coincidence Spectra for CH₄ Source Gas

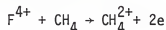
1. Primary ions detected



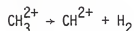
2. Single or multiple charge exchange of a primary ion



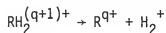
3. Creation of a molecular ion



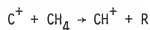
4. Decay of molecular ion



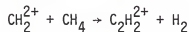
5. Coulomb explosion of a short-lived molecular ion



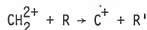
6. Protonation



7. Pickup of a carbon atom



8. Molecular dissociation through secondary collisions



Note: R denotes unidentified residual components and F⁴⁺ is the pump beam.

Figure 4. Synthetic spectrum based on model calculations.

creation have a characteristic "V-shaped" signature which extends above the primary ion analyzer voltage line and extends to shorter and longer times of flight than the primary ion of the same family of ions.

Given the insights provided by the computer model, consider the actual spectra. Figures 5, 3 and 6 are spectra from CH_4 gas at pressures of 0.5 mtorr, 1.0 mtorr and 4.0 mtorr, respectively. There are several regions of interest in each of these spectra. These regions have been identified as windows in the spectra and have been expanded to reveal greater detail.

Window 0 in Figure 7 displays the ions of the form CH_n^+ and their associated loci. Figure 8 is the projection of the TOF dimension of the ions CH_4^+ , CH_3^+ , CH_2^+ , CH_1^+ and C^+ , as well as the peaks for the contaminant molecules H_2O^+ (which may contain counts from undifferentiated CH_6^+ ions), OH^+ (with undifferentiated CH_5^+ ions) and an unidentified contaminant of $M/q = 20$.

The presence of loci beneath the line of primary ions is an indication of the decay of some heavier ion to the species associated with a particular locus. The loci of the singly charged ions are not well resolved at this time, but do suggest the presence of larger hydrocarbon ions.

Window 1 and its attendant projections (Figures 9 and 10) display ions of the form CH_n^{2+} and CH_n^{3+} . Eight peaks are indicated in this spectrum. They result from the detection of CH_4^{2+} , CH_3^{2+} , CH_2^{2+} , CH^{2+} , C^{2+} , CH_4^{3+} , CH_2^{3+} and C^{3+} ions. The C^{2+} and C^{3+} , like the C^+ , are stable atomic primary ions.

The current measurements present the first direct observation of the CH_4^{2+} molecular ion without doing charge stripping as reported by Ast, et al.³ The fact that we see CH_4^{2+} and CH_2^{2+} as peaks in the time-of-flight dimension indicates that their lifetimes are $\tau \geq 3 \mu\text{s}$, the instrumental flight time for these ions. Similarly these measurements present the first observation of CH^{2+} molecular ions. As in the case of the CH_4^{2+} and CH_2^{2+} ions

Figure 5. Recoil spectrum of CH_4 at a target gas pressure of 0.5 mtorr.

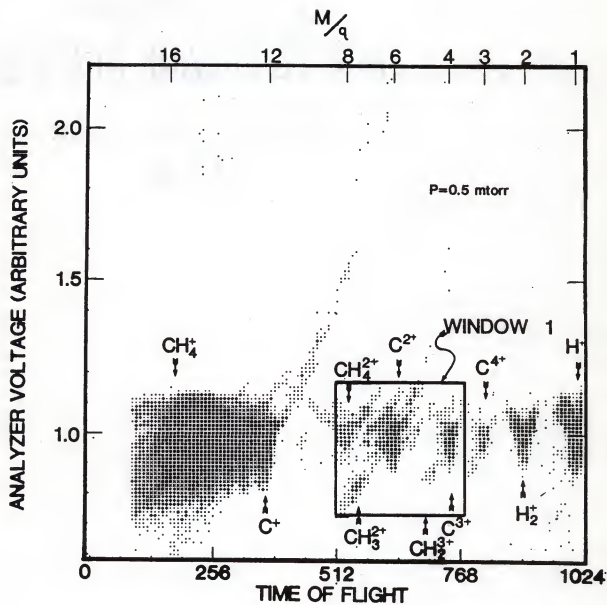


Figure 6. Recoil spectrum of CH_4 at a target gas pressure of 4.0 mtorr.

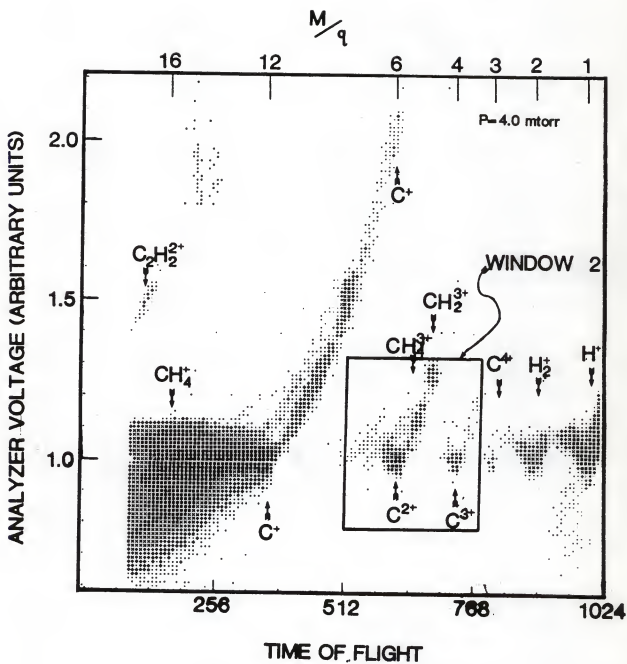


Figure 7. Window 0, showing ions of the form CH_n^+ originating from 1.0 mtorr of CH_4 gas.

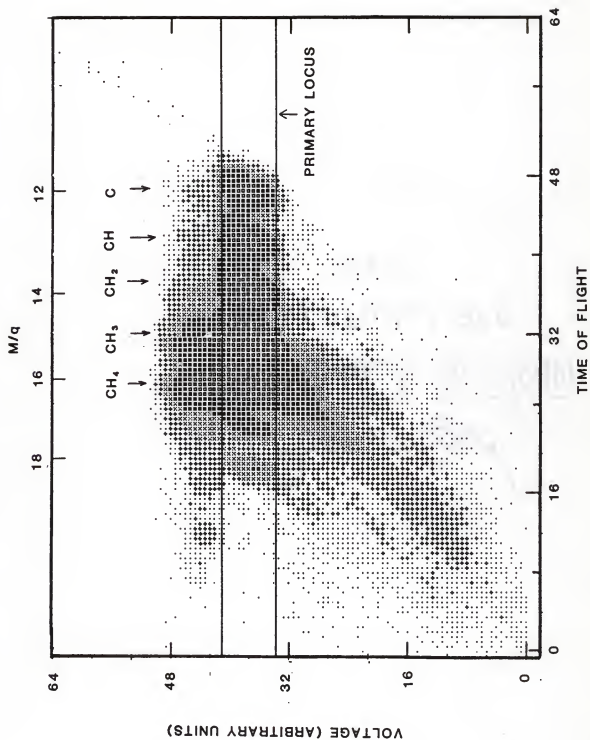


Figure 8. Projection of primary ion locus from window 0.

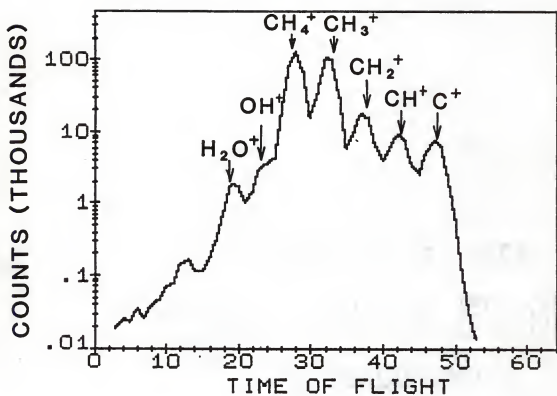


Figure 9. Window 1, showing ions of the form CH_n^{2+} and CH_n^{3+} originating from 0.5 mtorr of CH_4 gas.

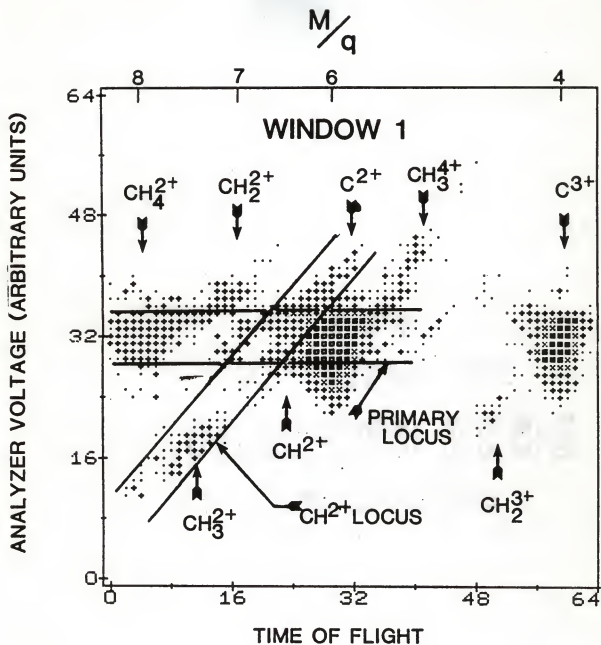
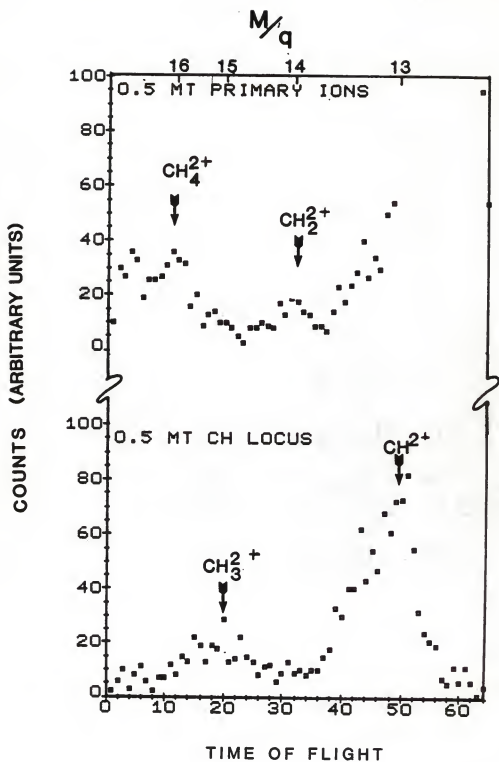


Figure 10. Projections of the primary ion locus and CH^{2+} locus from window 1.



the CH^{2+} species is estimated to have a lifetime, $\tau \sim 3 \mu\text{s}$. Lying below the primary ion locus are two peaks identified as CH_3^{2+} and CH_2^{3+} . These data represent the first observations of these species. It is seen that there is essentially no intensity on the primary ion locus for these two groups. Model calculations indicate that these two ion species were formed in primary collisions with the pump beam and accelerated out of the ion source. Their lifetimes are short compared to the instrumental flight time of $\sim 3 \mu\text{s}$; the CH_3^{2+} and CH_2^{3+} decay in flight to CH^{2+} and C^{3+} , respectively. Because they are peaks in the time-of-flight dimension their lifetimes must be comparable to their respective acceleration times in the recoil ion source. Hence a limit of $\tau \sim 200 \text{ ns}$ is established for the lifetimes of CH_3^{2+} and CH_2^{3+} . Also seen in Window 1 above the primary locus are three continua, one of which contains a peak corresponding to CH_4^{3+} decaying in flight to C^{2+} . The lifetime for the CH_4^{3+} ion is approximately the acceleration time, $\tau \approx 200 \text{ ns}$.

It is worthwhile to note that the number of coincidence counts stored in Fig. 5 for the main spectrum is $> 4 \times 10^6$ counts. The projections in Fig. 10 show that the intensity in the peaks of interest (CH_4^{2+} , CH_2^{2+} , CH_3^{2+} , CH^{2+}) are an extremely small part of the total coincidence intensity. If one performed a one dimensional standard dispersive analysis, such small signal intensities would be lost in the noise.

Figure 6 depicts the spectrum for CH_4 at a pressure of 4.0 mtorr. That the processes involved in producing these molecular ions are very pressure dependent is immediately apparent on comparison with the 0.5 mtorr spectrum. In window 2, shown in Figure 11, all intensity below the primary ion locus is absent in contrast to the features noted for window 1 at the lower source pressure. Furthermore the CH_4^{2+} , CH_3^{2+} and CH_2^{2+} ions have been displaced from the window to the C^+ locus which is outside of the boundaries of the window.

Figure 11. Window 2, showing ions of the form CH_n^{2+} and CH_n^{3+} originating from 4.0 mtorr of CH_4 gas.

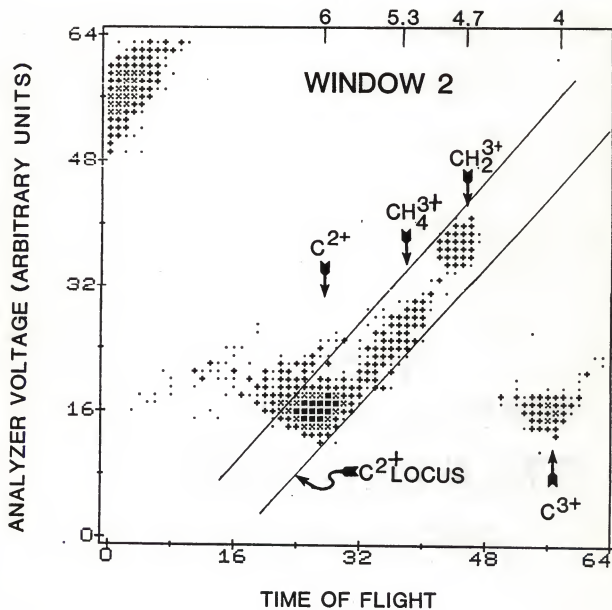
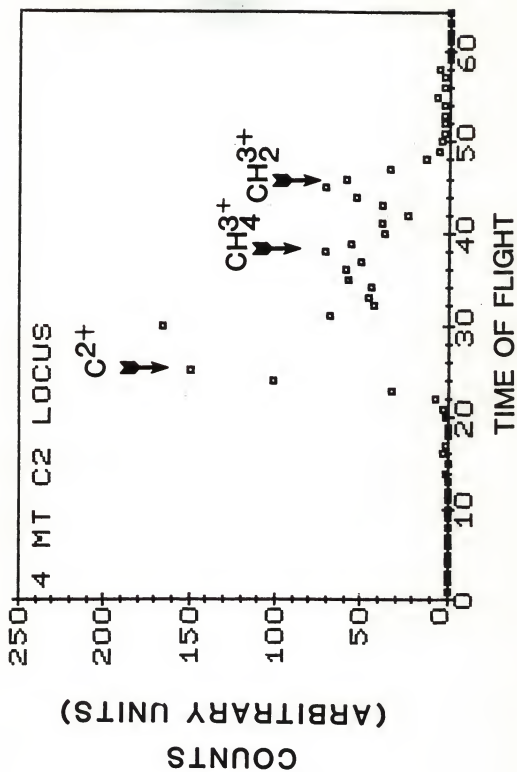
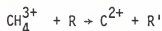


Figure 12. Projection of the C^{2+} locus from window 2.



This displacement is the result of secondary collisions at the higher source pressure. The CH_2^{3+} ions seen below the primary ions locus in window 1 are absent in window 2. However we see strong intensities for CH_4^{3+} and CH_2^{3+} in the C^{2+} locus indicated in window 2. These two molecular ion species are clearly seen in the projection of the 4.0 mtorr C^{2+} locus of Fig. 12. We do not detect them as CH_4^{3+} and CH_2^{3+} , but see the dissociation products of the reactions



and



where R and R' are unidentified components. The fact that CH_4^{3+} is a sharp peak as shown in the projection of the C^{2+} locus as given in Fig. 12 indicates that the lifetime for this species is comparable to the acceleration time, $\tau \approx 200$ ns. This lifetime limit could be increased as there is competition between the dissociation rate and the natural decay rate at this source pressure. The same conclusions can be made for the CH_2^{3+} ion species in view of the data of windows 1 and 2.

To the far right of each spectrum are peaks produced by the detection of H_2^+ and protons. These have a characteristic "V" shape that is attributed to a "Coulomb explosion" or exoergic decay of a molecule near the site of its creation. The symmetry of the "V" shape is believed to be due to the fact that only those fragments of the explosion that are projected in the forward or backward direction relative to the usual trajectory of the molecule survive the collimation and are detected. Model calculations show the height of the feature is determined by the energy released in the explosion and that the maximum Q-value for these events is < 10 eV. This conclusion is in agreement with the work of Edwards, et al.,¹⁵ which has peaks near 5 eV

in the energy spectrum of H^+ and H_2^+ from $O^+ \rightarrow CH_4$ collisions. This characteristic signature is also seen for the CH_4^{2+} ion in the 0.5 mtorr data, but the mechanism for how the feature is produced here is not now clear. A Coulomb explosion of CH_4^{2+} would necessarily have to involve an unidentified partner of mass comparable to CH_4^{2+} given the time spread in the branches of the explosion seen in Figure 4.

Returning again to Figure 3, there is a region corresponding to ions having M/q greater than that of CH_4^+ . On the left hand side of the spectrum there are peaks associated with the background gas contaminants O_2^+ and N_2^+ . There is also a peak at M/q of ~ 28 on the locus of CH_n^+ ions, indicating the formation of heavier hydrocarbon ion species such as $C_2H_2^+$, $C_2H_3^+$, and $C_2H_4^+$ which decay into lighter, as yet unidentified, CH_n^+ ion species. Lastly, primary ions of M/q of about 40 and 44 plus an unusual horizontal locus lying above the primary ion locus in this region exist, but also remain unidentified at present.

The detection of molecular ions of mass greater than that of the initial CH_4 molecule suggest that there is collisional chemistry taking place in the gas cell. These chemically reactive events are happening very near the site of the pump beam-target gas collisions because the molecules thus formed receive the full acceleration of the extraction potentials and appear as peaks in their locus. This implies that the reactions occur in collisions with energy of only a few eV.

Finally, care has been taken to insure that none of the foregoing spectral features could be due to contaminant isotopes (such as ^{13}C). There are no peaks observed in any of the spectra indicating the presence of ^{13}C primary ions or of any primary molecular ion containing that isotope. Furthermore, spectra have been taken using $^{13}CH_4$ which show the same features as the $^{12}CH_4$ spectra, shifted in TOF due to the mass difference.

Chapter V

CONCLUSIONS AND PROSPECTS

The new technique of molecular ion recoil spectroscopy has been favorably applied to produce multiply charged molecular ions and to observe collisional chemistry on an event-by-event basis. By bombarding methane with high energy heavy ions and analyzing the recoil products both in time of flight and in charge state, many new molecular ions and chemical processes have been discovered. The first observation of CH^{2+} and CH_3^{2+} has been made, as has the first observation of any trebly charged molecules, CH_4^{3+} and CH_2^{3+} . Several dissociation pathways of the various metastable molecular ions have been discerned and lifetime estimates made. Ion species such as CH_3^{2+} , CH_4^{3+} and CH_2^{3+} exhibit lifetimes > 200 ns. Previous theoretical model structure calculations by Pople, *et al.*⁸ have suggested that CH^{2+} had no bound states and that CH_3^{2+} should have an extremely short lifetime. The data indicates otherwise. The recent theoretical work by Heil, *et al.*⁹ for CH^{2+} shows a shallow minimum in the molecular potential for the diabatic $2\Sigma^+$ state, but no lifetime estimates were made. No theoretical calculations for the lifetimes of CH_4^{3+} or CH_2^{3+} exist.

It is also clear that chemical reactions involving many collisions between reactants are occurring, yielding species such as C_2H_2^+ and others of even greater mass.

The potential for further application of this technique is enormous. Work is in progress to improve the time resolution and recoil ion intensity of the present system by designing a new ion source with optimal optics. These modifications should make possible improvements in the statistics of

high charge state molecules and clearer definition of the loci. This would permit such experiments as determining the pressure dependences (and thus collisional history) of some of the chemical reactions and determining the end products of the decay of $C_2H_n^+$ ions. The striking differences in the dissociation path taken by ions such as CH_2^{3+} as the target pressure changes are also ground for further study.

There should also be sufficient brightness of recoil ions for them to be collimated into beams. This opens the door to detailed studies of any of the recoil ions and their processes. Immediate plans along this line call for extracting the various unidentified higher mass ions and fragmenting them in a secondary gas cell. It is hoped that identification of the fragments will permit identification of their parents.

This technique is certainly not limited to recoils from methane; we have already applied it to targets of water vapor and to mixtures of gasses such as N_2 and deuterium, D_2 . These spectra are just as rich in new molecular ions and new processes as the CH_4 spectra, with the $N_2 + D_2$ mixture producing particularly interesting chemical reactions.

It is hoped that many new physical insights into the nature of the molecule can be made with molecular ion recoil spectroscopy, insights bridging the disciplines of physics and chemistry. Each has much to learn from the other.

APPENDIX A

Derivation of the Spectrum Model

A schematic diagram of the recoil ion source and analysis system appears in Figure A1. The geometry of the acceleration region has been simplified from that shown in Figure 1 to just three grids which form two field regions. These grids are held at voltages V_B , V_1 and ground, which establishes a potential V_0 at the location of the pump beam.

The goal of the model is to predict the time of flight and analyzer voltage of ions detected after traversing this system. There are five types of events which can happen to an ion prior to detection:

- 1) If nothing happens to an ion formed at the pump beam, it is detected as a primary ion.
- 2) The ion may undergo charge exchange.
- 3) The ion may decay to a light mass.
- 4) The ion may capture another fragment and increase its mass.
- 5) An unstable molecule may Coulomb explode near the pump beam.

Consider the fundamental physics of each of these possibilities:

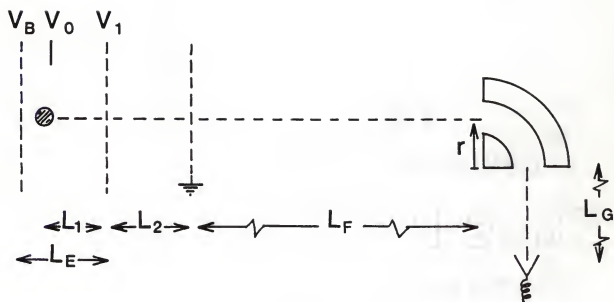
1) Primary Ions

An ion of charge q and mass m formed at the beam will be accelerated to a final energy of

$$E = q(V_0 - B_1) + qV_1$$

The work done on the ion in each field region will yield the acceleration.

Figure A1. Schematic diagram of the ion source and analysis system.



$$mA_1L_1 = q(V_0 - V_1)$$

$$mA_2L_2 = qV_1$$

$$A_1 = \frac{q(V_0 - V_1)}{mL_1}$$

$$A_2 = \frac{qV_1}{mL_2}$$

The time of flight through the ion source can now be found from

$$Z = v_0 t + 1/2 at^2$$

giving

$$t = \frac{-v_0 \pm \sqrt{v_0^2 + 2aZ}}{a}$$

The negative branch is rejected as unphysical, since time cannot be negative. The initial velocity of the ion in the first stage is zero, and the velocity as it enters the second stage is easily found from its energy. The time to clear each stage is thus

$$T_1 = \sqrt{\frac{2L_1}{A_1}} \quad T_2 = \frac{-v_0 + \sqrt{2A_2L_2}}{A_2}$$

This leaves only the drift time. The final velocity of the ion is found from its energy. The time to traverse the space to the analyzer, pass through the analyzer and be detected is

$$T_F = (L_F/V_F) + (\pi r/2V_F) + (L_G/V_F)$$

giving a total time of flight of

$$T = T_1 + T_2 + T_F$$

The analyzer voltage can be calculated directly from the relation

$$V = \frac{kE}{q}$$

where k is a geometrical constant of the analyzer.

2) Charge Exchange

The effect of a charge-changing reaction is modeled by changing q to q' for all calculations of events occurring after the reaction. In order to determine the effect of any sort of reaction which might occur anywhere along the flight path, the parameter x is introduced. This parameter is the distance to the site of the reaction from the pump beam. Calculations made will now have three parts. For reactions in the first acceleration stage, the ion will approach the reaction's location, react and escape the first stage and then traverse the second stage. In second stage reactions, the ion must clear the first stage, approach the reaction's location, then react and escape the second stage. Analogously to the primary ion case, the relevant equations are, for the first stage,

$$E = \left[\frac{q(V_0 - V_1)x}{L_1} \right] + \left[\frac{q'(V_0 - V_1)(L_1 - x)}{L_1} \right] + (q'V_1)$$

$$A_1 = \frac{q(V_0 - V_1)}{mL_1} \quad A_2 = \frac{q'(V_0 - V_1)}{mL_1} \quad A_3 = \frac{q'V_1}{mL_2}$$

$$T_1 = \sqrt{\frac{2x}{A_1}} \quad T_2 = \frac{-v_{01} + \sqrt{v_{01}^2 + 2A_2(L_1 - x)}}{A_2}$$

$$T_3 = \frac{-v_{02} + \sqrt{v_{02}^2 + 2A_3L_2}}{A_3}$$

and in the second stage,

$$E = \left[q(V_0 - V_1) \right] + \left[\frac{qV_1(x - L_1)}{L_2} \right] + \left[\frac{q'V_1(L_1 + L_2 - x)}{L_2} \right]$$

$$A_1 = \frac{q(V_0 - V_1)}{mL_1} \quad A_2 = \frac{qV_1}{mL_2} \quad A_3 = \frac{q'V_1}{mL_2}$$

$$T_1 = \sqrt{\frac{2L_1}{A_1}} \quad T_2 = \frac{-v_{01} + \sqrt{v_{01}^2 + 2A_2(x - L_1)}}{A_2}$$

$$T_3 = \frac{-v_{02} + \sqrt{v_{02}^2 + 2A_3(L_1 + L_2 - x)}}{A_3} .$$

The drift time is calculated in the same way as it was before. The analyzer voltage becomes

$$V = \frac{kE}{q^+} .$$

3) Decay

Should a molecular ion decay, its mass will change from m to m' . The daughter fragments will have the same velocity as the parent. If the decay happens in the drift space, no change in time of flight occurs, but the change in energy due to the mass change will alter the analyzer voltage. If the decay occurs in an acceleration stage, the accelerations imposed subsequent to the decay will be altered by the new mass.

The change in energy is handled by introducing a kinematic factor K_D which is subtracted from the total energy. The factor is the amount of kinetic energy lost due to the loss of mass. If the initial energy is

$$E_0 = 1/2 mv^2$$

and the final energy is

$$E_f = 1/2 m'v^2$$

then

$$K_D = E_i - E_f = \frac{1}{2} (m - m')v^2$$

or

$$K_D = \frac{(m - m')}{m} E_0 .$$

4) Pick-Up

In the opposite problem to the above, an ion captures, or picks up, another atom or molecular fragment. The mass now increases from m to m' . Treated as a totally inelastic collision with a stationary target, the velocity of the new projectile can be found from the conservation of momentum.

$$P_0 = mv = P_F = m'v'$$

$$v' = (m/m')v$$

The new projectile's energy is thus

$$E_f = 1/2 m'v'^2 = 1/2 m'(m/m')^2 v$$

or

$$E_f = (m/m')E_0$$

Another kinematic factor, K_p , is defined as the energy lost in the pick-up reaction.

$$K_p = E_0 - E_f = E_0 - (m/m')E_0$$

or

$$K_p = (1 - m/m')E_0$$

The change of both energy and velocity means both time of flight and analyzer voltage will be affected. The final expressions for all possible events so far considered are, for first stage reactions,

$$E = \left[\frac{q(V_0 - V_1)x}{L_1} \right] + \left[\frac{q'(V_0 - V_1)(L_1 - x)}{L_1} \right] + q'V_1 - K_D - K_p$$

decay being exoergic. Here that topic is taken up by assuming that such events result from unstable molecular structures and therefore happen near the molecule's point of creation (i.e., at the pump beam).

The conservation of energy and momentum for an energetic decay of a molecule of mass m into fragments of masses m' and $(m-m')$ states

$$1/2 mv^2 = 1/2(m-m')v_1^2 + 1/2 m'v_2^2 - Q$$

$$mv = (m-m') v_1 + m'v_2$$

where Q is the exoergicity of the reaction. This system of equations is easily solved, giving

$$v_2 = v \pm \sqrt{\frac{2(m-m')Q}{mm'}}$$

$$v_1 = \frac{mv - m'v_2}{(m-m')}$$

The ejected fragment of mass m' and velocity v_2 may be cast in the forward or backward direction, as indicated by the choice of sign. In the case of forward scattering the ion escapes the source with the extra energy and velocity imparted by the explosion. The backward scattering drives the fragment deeper into the source. This fragment then escapes with a higher energy due to its being deeper in the extraction field, but with longer time of flight due to the extra distance it travelled. This effect gives rise to the characteristic "V" shaped signature referred to earlier.

The forward scattered fragment is treated by the model exactly as an ordinary decay save that rather than losing energy, it gains. This means that

$$E = 1/2 m'v_2^2 + q'(V_0 - V_1) + q'V_1$$

$$A_1 = \frac{q(V_0 - V_1)}{mL_1} \quad A_2 = \frac{q'(V_0 - V_1)}{m'L_1} - \frac{K_p}{m'(L_1 - X)} \quad A_3 = \frac{q'V_1}{m'L_2}$$

$$T_1 = \sqrt{\frac{2x}{A_1}} \quad T_2 = \frac{-v_{01} + \sqrt{v_{02}^2 + 2A_2(L_1 - x)}}{A_2}$$

$$T_3 = \frac{-v_{02} + \sqrt{v_{02}^2 + 2A_3L_2}}{A_3}$$

and in the second stage,

$$E = \left[q(V_0 - V_1) + \frac{qV_1(x - L_1)}{L_2} \right] + \left[\frac{q'V_1(L_1 + L_2 - x)}{L_2} \right] - K_D - K_p$$

$$A_1 = \frac{q(V_0 - V_1)}{mL_1} \quad A_2 = \frac{qV_1}{mL_2} \quad A_3 = \frac{q'V_1}{m'L_2} - \frac{K_p}{m'(L_1 + L_2 - x)}$$

$$T_1 = \sqrt{\frac{2L_1}{A_1}} \quad T_2 = \frac{-v_{01}^2 + \sqrt{v_{01}^2 + 2A_2(x - L_1)}}{A_2}$$

$$T_3 = \frac{-v_{02} + \sqrt{v_{02}^2 + 2A_3(L_1 + L_2 - x)}}{A_3}$$

and the analyzer voltage will again be

$$V = \frac{kE}{q'}$$

The model performs these calculations at intervals of X ranging from $X=0$ to $X=(L_1+L_2+L_F)$. It is by virtue of these reactions taking place over a continuum of locations that continuous features like the charge exchange loci are produced. The ions are accelerated different distances as different species, resulting in loci branching off the primary ion peaks in the spectrum.

5) Coulomb Explosions

The foregoing discussion of decay neglected the possibility of the

and

$$A_2 = \frac{(1/2 m' v_2^2)}{m' L_1} + \frac{q'(V_0 - V_1)}{m' L_1}$$

while all other expressions remain the same.

It has been assumed in this discuss that $X=0$ and therefore $v=0$. The actual model allows X to vary for future studies, but all results presented in this work assume $X=0$.

The case of backward scattering first calculates the distance the fragment penetrates into the source by equating the extraction field energy to the ion's explosion energy:

$$\frac{q'(V_B - V_1)}{L_E} Y = 1/2 m' v_2^2 = E_1$$

$$Y = \frac{E_1 L_E}{q'(V_B - V_1)} .$$

If Y exceeds the depth of the source, the ion is assumed to be lost.

Otherwise, the ion is allowed to accelerate out of the source in the usual fashion. This makes

$$E = \frac{q'(V_B - V_1)(L_1 + Y)}{L_E} + q'V_1$$

$$A_2 = \frac{2E_1}{m'Y}$$

$$A_3 = \frac{q'(V_B - V_1)}{m' L_E}$$

$$A_4 = \frac{q'V_1}{m' L_2}$$

$$T_1 = \sqrt{\frac{2Y}{A_2}}$$

$$T_2 = \sqrt{\frac{2(L_1 + Y - X)}{A_3}}$$

$$T_3 = \frac{-v_0 + \sqrt{v_0^2 + 2A_4 L_2}}{A_4}$$

The drift time and analyzer voltage expressions remain the same as always.

These expressions are evaluated over a range of Q -values from $Q=0$ to some maximum that is entered as data. As Q is increased, the height of the branches in the spectrum increases. By comparing these model spectra

to the data, approximations of the Q-values of the actual reactions can be made.

APPENDIX B

Computer Programs

This section contains the BASIC language program codes of three programs. The first is a routine for producing two-dimensional plots of the data provided by the model calculations. It is a modification of the scientific plotting program SCIPLOT, originally by Paul Warne and modified by James Legg. The second program, SPECTRA MODEL, is a subroutine for the first that models spectra of primary ions, charge exchange and mass changing reactions. The last program is the model of Coulomb explosions and is therefore called COULOMB EXPLOSION.

PLOT2D (SCIPLLOT, as modified)

```

5 HIMEM 36735: LOMEM: 24576
10 CD$ = CHR$(4): IF PEEK(36736) + PEEK(38399) < > 96 THEN PRINT CD$;
"BL0AD PKWDATA,A36736"
13 DIM D(1024),Y0(2),Y1(2),MY(2),IN$(20),PC(64),JLIM(2)
15 POKE 232,128: POKE 233,143
20 SCALE= 1: ROT= 0
25 D2$ = "D2":D1$ = "D1"
96 HGR : HGR2 : TEXT : HOME
97 DEF FN XN(X) = (X - X0) * XX + XL
98 DEF FN YN(Y) = (Y - Y0(IJ)) * YY + YB
99 POKE 51,0: ONERR GOTO 3100
100 XL = 18:XR = 278:YB = 167:YT = 23: HCOLOR= 3:
110 Y0(1) = - 1:Y0(2) = 29:Y1(1) = 35:Y1(2) = 65:MY(1) = 0:MY(2) = 32
130 FOR IJ = 1 TO 2
140 POKE 230,32: IF IJ = 2 THEN POKE 230,64
160 HPL0T XL,YB TO XR,YB:X0 = - 1:X1 = 64:MX = 0:IX = 16:XX = 4:YF = 176:Y2
= 0:JX = 8
300 FOR X2 = MX TO X1 STEP IX:Y3 = YF + Y2:Y2 = - Y2:X3 = FN XN(X2)
305 DRAW 2 AT X3,YB: GOSUB 2310: NEXT X2
380 FOR X2 = MX - (JX * INT((MX - X0) / JX + .1)) TO X1 STEP JX: DRAW 1 AT
FN XN(X2),YB: NEXT : TEXT
390 I = 2
400 YY = - 4:MY = MY(IJ):Y0 = Y0(IJ):Y1 = Y1(IJ)
430 HPL0T XL,YB TO XL,YT TO XR,YT TO XR,YB
530 GOSUB 2200: FOR Y2 = MY TO Y1 STEP IX:Y3 = FN YN(Y2): DRAW 2 AT XL,Y3:
GOSUB 2540: NEXT Y2
610 FOR Y2 = MY - (JX * INT((MY - Y0) / JX)) TO Y1 STEP JX: DRAW 1 AT XL,
FN YN(Y2): NEXT Y2: TEXT
650 NEXT IJ
670 RG$ = ""
700 GOSUB 5000
800 IP = 0:S = 4:S$ = "USE LETTERS OR PLOT SYMBOLS?":RG$ = "L,F": GOSUB 2000:
IF IN$(S) = "L" THEN IP = 1
810 S = 5:S$ = "WHAT PLOT CHARACTER?":RG$ = "": GOSUB 2000: IF IP = 0 THEN SY
= V0
820 IF IP = 1 THEN X2$ = IN$(S)
950 II = 1
1000 FOR I = 1 TO D(0) STEP 2
1005 XP = D(I):YP = D(I + 1)
1010 IF XP < 0 OR XP > 64 THEN II = 1: GOTO 1100
1015 IF YP < 0 OR YP > 64 THEN II = 1: GOTO 1100
1020 IF YP < 31.5 THEN 1050
1030 IF II < > 3 THEN IJ = 2: GOSUB 2200: POKE 230,64
1040 Y3 = FN YN(YP):X3 = FN XN(XP): IF IP = 0 THEN DRAW 17 AT X3,Y3:YS =
INT((SY - 1) / 4): FOR IM = (4 * YS + 1) TO SY: DRAW IM AT X3,Y3: NEXT IM: G
OTO 1100
1045 GOSUB 2330: GOTO 1100
1050 IF II < > 2 THEN IJ = 1: GOSUB 2200: POKE 230,32
1060 Y3 = FN YN(YP):X3 = FN XN(XP): IF IF = 0 THEN DRAW 17 AT X3,Y3:YS =
INT((SY - 1) / 4): FOR IM = (4 * Y3 + 1) TO SY: DRAW IM AT X3,Y3: NEXT IM: G
OTO 1100
1070 GOSUB 2330
1100 NEXT I

```

```

1965 TEXT
1970 S = 10:S$ = "MORE ON THIS GRAPH?" :RG$ = "Y:N": GOSUB 2000: IF IN$(S) = "
Y" GOTO 670
1997 S = 2:S$ = "ANOTHER GRAPH":RG$ = "Y.N": GOSUB 2000: IF IN$(S) = "Y" GOTO
96
1999 PRINT CD$;"RUN MENU, ";D1$
2000 PRINT S$;"( ";RG$;" )"? <" ;IN$(S);" )"; GOSUB 2800:OK = 0: IF A > 0 THEN I
N$(S) = A$: GOTO 2020
2305 A = LEN (IN$(S)): IF A = 0 GOTO 2090
2010 FOR I = 1 TO A: IF MID$(IN$(S),I,1) = "," THEN B = I + 1
2015 NEXT
2020 L = LEN (RG$): IF L = 0 GOTO 2095
2030 R$ = "":R = 0: FOR J = 1 TO L
2035 IF MID$(RG$,J,1) < " " THEN R$ = R$ + MID$(RG$,J,1): IF J < L GO
TO 2080
2040 IF VAL (R$) = 0 AND ASC (R$) < " " 48 GOTO 2060
2042 IF R = 0 THEN V0 = VAL (IN$(S)): IF V0 < VAL (R$) GOTO 2070
2044 IF R = 1 THEN IF V0 > VAL (R$) GOTO 2070
2046 IF R = 2 THEN VU = VAL ( MID$(IN$(S),B)): IF VU < VAL (R$) GOTO 2070

2048 IF R = 3 THEN IF VU > VAL (R$) GOTO 2070
2050 R = R + 1:OK = 1:R$ = "": GOTO 2080
2060 IF IN$(S) < " " R$ THEN R$ = "": GOTO 2080
2065 OK = 1: GOTO 2075
2070 OK = 0
2075 J = L
2080 NEXT
2090 IF OK = 0 THEN PRINT CHR$(7);"INVALID ENTRY; CHECK (RANGE)":AUT = 0:
GOTO 2000
2095 V0 = VAL (IN$(S)): RETURN
2100 I = I + 1:V0 = I
2110 I = I + 1: IF I > (A) THEN J = I:I = I - 1: GOTO 2120
2115 C = ASC ( MID$(A$,I,1)): IF C > 47 AND C < 58 GOTO 2110
2116 J = I
2120 V0 = VAL ( MID$(A$,V0,J - V0)): RETURN
2200 POKE - 16304,0: POKE - 16300,0: IF IJ = 2 THEN POKE - 16299,0
2210 RETURN
2310 X2$ = STR$(X2)
2330 L = LEN (X2$): IF X3 > 270 THEN X3 = 280 - 8 * L: GOTO 2340
2335 X3 = X3 - 4 * L
2340 DRAW ASC (X2$) AT X3,Y3: IF L = 1 GOTO 2360
2350 FOR I = 2 TO L: DRAW ASC ( MID$(X2$,I,1)): NEXT I
2360 RETURN
2540 Y2$ = STR$(Y2)
2570 L = LEN (Y2$):Y3 = Y3 + 3:X3 = XL - 2 - 8 * L
2572 IF Y3 > YB THEN Y3 = YB
2575 DRAW ASC (Y2$) AT X3,Y3: IF L = 1 GOTO 2590
2580 FOR I = 2 TO L: DRAW ASC ( MID$(Y2$,I,1)): NEXT I
2590 RETURN
2600 IF CV = 1 THEN PRINT CHR$(9)"GD": RETURN
2605 IF CV = 2 THEN PRINT CHR$(9)"G2D": RETURN
2610 RETURN
2800 A = 0:B = 0:A$ = ""
2810 GET C$:C = ASC (C$): IF C > 31 GOTO 2880

```

```

2815 IF C < > 8 GOTO 2820
2816 PRINT C$; IF A < 2 GOTO 2800
2818 A = A - 1:A$ = LEFT$(A$,A): GOTO 2810
2820 IF C = 13 THEN PRINT : RETURN
2826 IF C = 2 THEN 96
2828 IF C = 4 THEN PRINT : PRINT CD$,A$: POP : GOTO 2000
2829 IF C = 5 THEN STOP : RETURN
2830 IF C = 7 THEN GET IJ: GOSUB 2200: GOTO 2810
2840 IF C = 20 THEN TEXT : GOTO 2810
2850 IF C = 24 THEN PRINT CHR$(92): GOTO 2800
2852 IF C = 16 THEN GET C$: PRINT : PRINT CD$ + "PR# " + C$: GOTO 2810
2855 IF C = 26 THEN POP : POP : GOTO 1965
2857 IF C = 17 THEN GET CV: GOSUB 2600: GOTO 2810
2859 IF C = 18 THEN TEXT : PRINT : PRINT CD$;"RUN MENU";D$: END
2860 IF C = 25 THEN GOSUB 2900:C = LEN (A$):A$ = A$ + STR$(XC) + ",";B =
  LEN (A$) + 1:A$ = A$ + STR$(YC):A = LEN (A$): PRINT MID$(A$,C + 1);
2870 GOTO 2810
2880 IF C = 44 THEN B = A + 2
2890 PRINT C$;A = A + 1:A$ = A$ + C$: GOTO 2810
2900 GOSUB 2200: POKE 230,32: IF IJ = 2 THEN POKE 230,64
2905 XC = INT ( PDL (0) * 1.098): FOR I = 1 TO 10: NEXT :YC = INT ( PDL (1)
  * .75)
2910 XDRAW 2 AT XC,YC: FOR I = 1 TO 50: NEXT : XDRAW 2 AT XC,YC
2920 IF PEEK ( - 16384) < 128 GOTO 2905
2930 GET C$: TEXT : RETURN
2999 RETURN
3100 PRINT : PRINT CD$;"CLOSE ": TEXT : PRINT CD$;"PR#0": PRINT CHR$(7)"ERR
  OR " PEEK (222)" IN LINE " PEEK (218) + 256 * PEEK (219): GOTO 1965

```

SPECTRA MODEL

```

5000 REM THIS SUBROUTINE GENERATES MODEL 2-D SPECTRA
5030 JA = - 1:PI = 3.1416:LE = .00873:L1 = .00516:L2 = .00952 LF = .1:LG =
02:RA = .03:KA = 1:KT = - 2.95E07:KV = 0.245:CA = 148.5:CE = - 22:D(0) = 0
5040 VB = 175:VO = 150:V1 = 113.866:KD = 0:KP = 0
5080 RG$ = "D:C"
5090 S = 6:S$ = "DO YOU WISH TO PLOT DISCRETE OR CONTINUOUS EVENTS?": GOSUB 2
000:TYPE$ = IN$(S)
5095 RG$ = ""
5100 S = 7:S$ = "ENTER INITIAL CHARGE STATE": GOSUB 2000:QI = VO * 1.602E - 1
9
5110 S = 8:S$ = "ENTER FINAL CHARGE STATE": GOSUB 2000:QF = VO * 1.602E - 19
5120 S = 9:S$ = "ENTER INITIAL MASS": GOSUB 2000:MI = VO * 1.66E - 27
5130 S = 10:S$ = "ENTER FINAL MASS": GOSUB 2000:MF = VO * 1.66E - 27
5150 IF TYPE$ = "C" THEN 5290
5160 KD = 0:KP = 0
5190 RG$ = "B:D:A"
5200 S = 11:S$ = "DOES EVENT OCCUR AT BEAM, DURING ACCELERATION OR AFTER ACCE
LERATION?": GOSUB 2000:WHERE$ = IN$(S)
5210 IF WHERE$ = "B" THEN GOTO 5250
5220 IF WHERE$ = "D" THEN GOTO 5260
5230 IF WHERE$ = "A" THEN GOTO 5270
5240 JA = JA + 2:D(JA) = T * KT + CA:D(JA + 1) = V * KV + CB:D(0) = 2: RETURN
5250 QI = QF:MI = MF:X = 0: GOSUB 5390: GOTO 5240
5260 X = L1 + .001: GOSUB 5530: GOTO 5240
5270 X = L1 + L2 + LF / 2: GOSUB 5670: GOTO 5240
5290 REM THIS SECTION PRODUCES CONTINUOUS FEATURES
5310 FOR X = 1.0E - 4 TO (L1 + L2 + LF) STEP 5.0E - 4
5330 JA = JA + 2:KD = 0:KP = 0
5340 IF X < L1 THEN GOSUB 5390:D(JA) = T * KT + CA:D(JA + 1) = V * KV + CB:
D(0) = D(0) + 2
5350 IF X >= L1 AND X < (L1 + L2) THEN GOSUB 5530:D(JA) = T * KT + CA:D(J
A + 1) = V * KV + CB:D(0) = D(0) + 2
5360 IF X >= (L1 + L2) AND X <= (L1 + L2 + LF) THEN GOSUB 5670:D(JA) =
T * KT + CA:D(JA + 1) = V * KV + CB:D(0) = D(0) + 2
5375 NEXT X: RETURN
5390 REM FIRST ACCELERATION STAGE
5410 E0 = (QI * (VO - V1) * X) / L1
5420 IF MF < MI THEN KD = (E0 / MI) * (MI - MF)
5430 IF MF > MI THEN KP = E0 * (1 - MI / MF)
5460 A1 = QI * (VO - V1) / (MI * L1):A2 = QF * (VO - V1) / (MF * L1) - (KP /
MF * (L1 - X)):A3 = QF * V1 / (MF * L2)
5465 T = SQR (2 * X / A1)
5470 VZ = SQR (2 * E0 / MD):AZ = A2:LZ = (L1 - X): GOSUB 8000:T = T + TA
5475 E0 = E0 + (QF * (VO - V1) * (L1 - X) / L1) - KP
5480 VZ = SQR (2 * (E0 - KD) / MF):AZ = A3:LZ = L2: GOSUB 8000:T = T + TA
5485 EF = E0 + QF * V1: GOSUB 7000:T = T + TF
5490 E = EF - KD:V = (KA * E) / QF
5510 RETURN
5530 REM SECOND ACCELERATION STAGE
5550 E0 = QI * (VO - V1) + (QI * V1 * (X - L1) / L2)
5560 IF MF < MI THEN KD = (E0 / MI) * (MI - MF)
5570 IF MF > MI THEN KP = E0 * (1 - MI / MF)
5575 A1 = QI * (VO - V1) / (MI * L1):A2 = QI * V1 / (MI * L2):A3 = QF * V1 /
(MF * L2) - (KP / MF * (L2 - X + L1))

```

```

5580 E0 = GI * (VO - V1) : T = SQR (2 * L1 / A1)
5585 VZ = SQR (2 * E0 / MI) : AZ = A2 : LZ = (X - L1) : GOSUB 8000 : T = T + TA
5590 E0 = E0 + GI * V1 * (X - L1) / L2
5595 VZ = SQR (2 * E0 / MI) : AZ = A3 : LZ = (L1 + L2 - X) : GOSUB 8000 : T = T + T
A
5600 EF = E0 + (GF * V1 * (L1 + L2 - X) / L2) - KP : GOSUB 7000 : T = T + TF
5630 E = EF - KD : V = (KA * E) / GF
5650 RETURN
5670 REM DRIFT STAGE
5685 E0 = GI * (VO - V1) + GI * V1 : VI = SQR (2 * E0 / MI) : EF = E0
5690 IF MI > MF THEN KD = (E0 / MI) * (MI - MF) : GOTO 5700
5692 IF MI < MF THEN KP = E0 * (1 - MI / MF)
5695 A1 = GI * (VO - V1) / (MI * L1) : A2 = GI * V1 / (MI * L2)
5700 E0 = GI * (VO - V1) : T = SQR (2 * L1 / A1) : VF = SQR (2 * (EF - KD - KP)
/ MF)
5705 VZ = SQR (2 * E0 / MI) : AZ = A2 : LZ = L2 : GOSUB 8000 : T = T + TA
5710 T = T + (X - L1 - L2) / VI + (LF - X + L1 + L2) / VF + (PI * RA / (2 * V
F)) + (LG / VF)
5730 E = EF - KD - KP : V = (KA * E) / GF
5740 RETURN
7000 VF = SQR (2 * (EF - KD) / MF) : TF = (LF / VF) + (PI * RA / (2 * VF)) + (
LG / VF) : RETURN
8000 TA = (- VZ + SQR (VZ ^ 2 + 2 * AZ * LZ)) / AZ : RETURN

```

COULOMB EXPLOSION

```

5000 REM THIS SUBROUTINE SIMULATES COULOMB EXPLOSIONS
5030 JA = - 1:PI = 3.1416:LE = .00873:L1 = .00516:L2 = .00952:LF = .1:LG = .0
2:RA = .03:KA = 1:KT = - 2.95E7:KV = 0.245:CA = 89.5:CB = - 22:D(0) = 0
5040 VB = 175:VO = 150:V1 = 113.866
5073 RG$ = ""
5075 S = 13:S$ = "ENTER Q VALUE": GOSUB 2000:Q = V0 * 1.602E - 19:QB = Q
5100 S = 7:S$ = "ENTER INITIAL CHARGE STATE": GOSUB 2000:QI = V0 * 1.602E - 19

5110 S = 8:S$ = "ENTER FINAL CHARGE STATE": GOSUB 2000:QF = V0 * 1.602E - 19
5120 S = 9:S$ = "ENTER INITIAL MASS": GOSUB 2000:MI = V0 * 1.66E - 27
5130 S = 10:S$ = "ENTER FINAL MASS": GOSUB 2000:MF = V0 * 1.66E - 27
5205 FOR QA = 0 TO QB STEP 5E - 20
5207 Q = QA:JA = JA + 2
5240 X = 0: GOSUB 5890
5251 D(JA) = T * KT + CA:D(JA + 1) = V * KV + CB:D(0) = D(0) + 2
5260 NEXT
5270 RETURN
5800 REM FORWARD SCATTERED FRAGMENTS
5890 E0 = QI * (VO - V1) * X / L1:V1 = SQR (2 * E0 / MI)
5900 VG = SQR (2 * (MI - MF)) * SQR (Q) / ( SQR (MI) * SQR (MF)):VF = V1 +
VG:E2 = MF * (VF ^ 2) / 2
5920 A1 = QI * (VO - V1) / (MI * L1):A2 = (E2 - E0) / (MF * (L1 - X)) + QF * (
VO - V1) / (MF * L1):A3 = QF * V1 / (MF * L2)
5930 TESC = SQR (2 * X / A1)
5932 VZ = SQR (2 * E0 / MI):AZ = A2:LZ = L1 - X: GOSUB 8000:TESC = TESC + TA
5934 E0 = E2 + (QF * (VO - V1) * (L1 - X) / L1)
5936 VZ = SQR (2 * E0 / MF):AZ = A3:LZ = L2: GOSUB 8000:TESC = TESC + TA
5938 EF = E0 + QF * V1:VW = KA * EF / QF: GOSUB 7000:TESC = TESC + TF
5940 D(JA) = TESC * KT + CA:D(JA + 1) = VW * KV + CB:D(0) = D(0) + 2
5942 REM BACKWARD SCATTERED FRAGMENTS
5945 E0 = QI * (VO - V1) * X / L1
5950 VF = V1 - VG:E3 = MF * (VF ^ 2) / 2:Y = 0: IF VF < 0 THEN Y = E3 * LE / (
QF * (VB - V1))
5965 IF Y > (X + LE - L1) THEN 7001
5970 EF = QF * (VB - V1) * (L1 - X + Y) / LE + (QF * V1)
5980 IF VF > 0 THEN EF = E3 + QF * (VO - V1) * (L1 - X) / L1 + (QF * V1)
5985 V = KA * EF / QF:A2 = 1:A3 = QF * (VB - V1) / (MF * LE): IF Y < > 0 THEN
5987
5986 IF VF > = 0 THEN 5988
5987 A2 = (2 * E3 - E0) / (MF * Y):A1 = QI * (VO - V1) / (MI * L1):A4 = QF * V
1 / (MF * L2): GOTO 6000
5988 A1 = QI * (VO - V1) / (MI * L1):A4 = QF * V1 / (MF * L2):A3 = A3 + (VG ^
2) / (2 * (L1 - X))
6000 T = SQR (2 * X / A1): IF Y = 0 THEN 6020
6005 VZ = - SQR (2 * E0 / MI):AZ = A2:LZ = Y: GOSUB 8000:T = T + TA
6010 T = T + SQR (2 * (L1 - X + Y) / A3)
6015 E0 = QF * (VB - V1) * (L1 - X + Y) / LE: GOTO 6030
6020 VZ = SQR (2 * E0 / MI):AZ = A3:LZ = L1 - X: GOSUB 8000:T = T + TA
6025 E0 = E3 + QF * (VO - V1) * (L1 - X) / L1
6030 VZ = SQR (2 * E0 / MF):AZ = A4:LZ = L2: GOSUB 8000:T = T + TA
6035 GOSUB 7000:T = T + TF:JA = JA + 2: RETURN
7000 VF = SQR (2 * EF / MF):TF = (LF / VF) + (PI * RA / (2 * VF)) + (LG / VF)
: RETURN
7001 T = 0:V = 0:JA = JA + 2: RETURN
8000 TA = (- VZ + SQR (VZ ^ 2 + 2 * AZ * LZ)) / AZ: RETURN

```

REFERENCES

1. J. H. Agee, J. B. Wilcox, L. E. Abbey and T. F. Moran, Chem. Phys. 61 (1981) pp. 171-179.
2. R. Spohr, T. Bergmark, N. Magnusson, L. O. Werme, C. Nordling and K. Siegbahn, Physica Scripta 2 (1970) p. 31.
3. T. Ast, C. J. Porter, C. J. Proctor, and J. H. Beynon, Chem. Phys. Lett. 78 (1981) pp. 439-441.
4. M. Rabrenovic, A. G. Brenton and J. H. Beynon, Int. Journal Mass Spec. Ion Phys. 52 (1983) pp. 175-182.
5. A. E. Litherland, Ann. Rev. Nucl. Part. Sci. 30 (1980) pp. 437-473.
6. A. W. Hanner and T. F. Moran, Org. Mass Spec., 16 (1981) p. 512.
7. Per E. M. Siegbahn, Chem. Phys. 66 (1982) pp. 443-452.
8. J. Pople, B. Tidor and P. Schleyer, Chem. Phys. Lett. 88 (1982) pp. 553-537.
9. T. G. Heil, S. E. Butler and A. Dalgarno, Phys. Rev. A 27 (1983) pp. 2365-2383.
10. T. J. Gray and C. L. Cocke, IEEE Trans. Nucl. Sci. 30 (1983) pp. 937-942.
11. C. L. Cocke, Phys. Rev. A 20 (1979) p. 749.
12. A. S. Schlachter, W. Groh, A. Müller, H. F. Beyer, R. Mann and R. E. Olson, Phys. Rev. A 26 (1982) p. 1373.
13. R. D. Macfarlane and D. F. Torgerson, Phys. Rev. Lett. 36 (1976) p. 486.
14. A. K. Edwards, R. M. Wood and M. F. Stever, Phys. Rev. A 15 (1977) p. 48.
15. A. K. Edwards, J. E. Graves, R. M. Wood and M. F. Stever, J. Chem. Phys. 69 (1978) pp. 1985-1988.

16. R. Mann, F. Folkmann, R. S. Peterson, Gy Szabo and K. O. Groeneveld,
J. Phys. B 11 (1978) p. 3045.
17. C. R. Vane, M. H. Prior and R. Marrus, Phys. Rev. Lett. 46 (1981)
p. 107.
18. C. Can, Ph.D. Dissertation (Kansas State University, 1983).
19. C. M. Schmeissner, M. S. Thesis (Kansas State University, 1983).

MOLECULAR ION RECOIL SPECTROSCOPY
APPLIED TO METHANE

by

VINCENT NEEDHAM
B.S., Kansas State University, 1982

AN ABSTRACT OF A MASTER'S THESIS

submitted in partial fulfillment of the
requirements for the degree

MASTER OF SCIENCE

Department of Physics
Kansas State University

1984

ABSTRACT

Molecular ion species of the form $C_n H_m^{q+}$ have been studied using a recoil ion source which is pumped by a pulsed 19 MeV F^{4+} ion beam. Simultaneous time-of-flight and electrostatic analysis was utilized to give mass and charge state information about the $F^{4+} + CH_4$ collision system. Two-dimensional spectra of the final charge state vs. time of flight are thus obtained. Model calculations identify events displayed in these spectra. Ions such as CH_4^{2+} , CH_3^{2+} , CH_2^{2+} , CH^{2+} , CH_4^{3+} , CH_2^{3+} and other heavier molecular ions have been observed. A number of decay pathways for these ions have been identified and limits have been set on the ions' lifetimes.